Comparison of Technetium-99m-HMPAO and Technetium-99m-ECD Cerebral SPECT Images in Alzheimer's Disease

Christopher H. van Dyck, C. Huie Lin, Eileen O. Smith, Gary Wisniewski, Janet Cellar, Rhonda Robinson, Meena Narayan, Alexandre Bennett, Richard C. Delaney, Richard A. Bronen and Paul B. Hoffer

Departments of Psychiatry, Neurology, and Diagnostic Radiology, Yale University School of Medicine, New Haven, Connecticut

SPECT has shown increasing promise as a diagnostic tool in Alzheimer's disease (AD). Recently, a new SPECT brain perfusion agent, ^{99m}Tc-ethyl cysteinate dimer (^{99m}Tc-ECD) has emerged with purported advantages in image quality over the established tracer, ^{99m}Tc-hexamethylpropyleneamine oxime (^{99m}Tc-HMPAO). This research aimed to compare cerebral images for ^{99m}Tc-HMPAO and ^{99m}Tc-ECD in discriminating patients with AD from control subjects. **Methods:** Twenty-four AD patients (mean age ± s.d. = 68.9 ± 8.2 yr) and 13 healthy subjects (68.4 ± 8.0 yr) were scanned sequentially with 20 mCi of each tracer using the CERASPECT system within 1 mo. Scanning began on average 11.5 ± 2.8 min after ^{99m}Tc-HMPAO injection and 41.8 ± 10.1 min after ^{99m}Tc-ECD. A ratio, *R*, was derived of count densities in "typically affected" brain structures (parietal and temporal association cortices) to "unaffected" structures (cerebellum, basal ganglia, thalamus, occipital cortex, and sensorimotor cortex). **Results:** Analysis of variance revealed significant interaction between diagnostic group and radiopharmaceutical ($F = 4.71$; $df = 1,35$; $p = 0.04$), with ^{99m}Tc-ECD demonstrating better separation of *R* values between AD patients and control subjects than ^{99m}Tc-HMPAO. Receiver operating characteristic (ROC) analysis revealed no significant difference in the ability of the two tracers to correctly classify AD patients and control subjects. Both tracers showed high diagnostic accuracy (^{99m}Tc-ECD: sensitivity = 100%, specificity = 92%; ^{99m}Tc-HMPAO: sensitivity = 100%, specificity = 85%). **Conclusion:** Technetium-99m-ECD shows greater contrast than ^{99m}Tc-HMPAO between affected and unaffected brain structures in AD when patients are compared to age-matched control subjects. Both tracers perform equally well in correctly classifying patients and control subjects.

Key Words: SPECT; Alzheimer's disease; technetium-99m-HMPAO; technetium-99m-ECD

J Nucl Med 1996; 37:1749–1755

SPECT has shown increasing promise as a diagnostic tool in Alzheimer's disease (AD). An abnormal pattern of perfusion (i.e., hypoperfusion of parieto-temporal association cortices) has been consistently reported by SPECT studies in AD patients (*1–5*). This pattern demonstrated by SPECT has a high predictive value for the presence of AD (*3*). Moreover, longitudinal data are unfolding which support the diagnostic accuracy of SPECT against the gold standard of histopathology at autopsy (*5–7*).

The ^{99m}Tc-based SPECT brain perfusion agents are more suitable for routine clinical use than those labeled with other isotopes (e.g., ^{123}I). Technetium-99m is a generator product which, when complexed with an appropriate chelate, forms a radiochemically pure and stable tracer. In comparison to ^{123}I, ^{99m}Tc confers more favorable dosimetry and does not require premedication for thyroid blockade. For many years, ^{99m}Tc-hexamethylpropyleneamine oxime (^{99m}Tc-HMPAO) (*8,9*) has been the only ^{99m}Tc-based brain perfusion agent commercially available in most countries. This tracer has greatly facilitated the routine assessment of cerebral perfusion in a variety of disorders. Recently, a second ^{99m}Tc-based agent, ^{99m}Tc-ethyl cysteinate dimer (^{99m}Tc-ECD; also known as ^{99m}Tc-bicisate) (*10–12*), was approved for clinical use in the United States. Whereas both ^{99m}Tc-HMPAO and ^{99m}Tc-ECD have been demonstrated to be markers of regional cerebral perfusion (*13–16*), some differences have emerged in their pharmacological behavior.

A systematic comparison of ^{99m}Tc-HMPAO and ^{99m}Tc-ECD in healthy human subjects was previously undertaken by Léveillé et al. (*17*). These investigators found the cerebral kinetics and initial distribution of ^{99m}Tc-HMPAO and ^{99m}Tc-ECD to be similar. After intravenous injection, both agents were rapidly taken up by the brain in proportion to cerebral blood flow and remained stable in distribution for several hours. The fraction retained in the brain was similar for both tracers. ^{99m}Tc-ECD was cleared from the blood more rapidly than ^{99m}Tc-HMPAO. The brain-to-soft-tissue activity ratios were higher for ^{99m}Tc-ECD and continued to increase with time. These factors may have contributed to the fact that ^{99m}Tc-ECD images were considered "easier to interpret" than those with ^{99m}Tc-HMPAO.

Comparative studies of these two tracers in neurological diseases are also necessary, since their pharmacokinetics may be altered by these states. Such comparisons have been largely limited to stroke (*18–22*) or brain tumor (*23*) and collectively indicate that ^{99m}Tc-ECD shows higher lesion-to-normal tissue contrast than ^{99m}Tc-HMPAO.

The only previous comparative studies of ^{99m}Tc-HMPAO and ^{99m}Tc-ECD in AD have used small numbers of AD patients combined with other neurological patients. Castagnoli et al. (*21*) compared image quality in 17 patients with dementia or chronic stroke, 5 of whom had probable AD. This report found that ^{99m}Tc-ECD demonstrated superior "image quality" and lesion-to-normal tissue contrast by ROI analysis compared to ^{99m}Tc-HMPAO. Pupi et al. (*22*) compared the regional steady-state influx constants (K_i) for the two tracers in five neurological patients, three of whom had probable AD, and found that they were closely correlated for several brain regions. Concentration of brain radioactivity was also found to be stable from 35 to 60 min postinjection for both tracers.

Comprehensive comparative studies of ^{99m}Tc-HMPAO and ^{99m}Tc-ECD in AD are essential, as these tracers will likely constitute the major tools for clinical SPECT rCBF studies for years to come. The present research used semiquantitative

Received Aug. 2, 1995; revision accepted Feb. 9, 1996.

For correspondence or reprints contact: Christopher H. van Dyck, MD, CB 2041, Yale University School of Medicine, 333 Cedar St. New Haven, CT 06520.

TABLE 1
Subject Characteristics

Variable	Alzheimer's (n = 24) Mean s.d.	Healthy (n = 13) Mean s.d.
Demographics		
Age (yr)	68.9 ± 8.2	68.4 ± 8.0
Gender	12 M, 12 F	8 M, 5 F
Handedness	23 R, 1 L	13 R
Education (yr)	14.5 ± 2.9	15.8 ± 3.7
Neuropsychological		
Ham-D	4.7 ± 2.9*	2.9 ± 2.1
MMSE	19.8 ± 3.4†	29.2 ± 1.1
DRS	106.3 ± 18.1†	139.3 ± 4.9
ADAS-Cog	24.5 ± 8.7†	5.1 ± 1.7
Verbal IQ	85.3 ± 12.6†	113.2 ± 17.4
Performance IQ	73.4 ± 14.1†	113.5 ± 15.0
Full Scale IQ	79.5 ± 12.3†	114.5 ± 17.3
Disease Characteristics		
Duration (mo)	48.8 ± 19.6	
Hachinski Score	0.6 ± 0.7	

*Differs from healthy control value, $p < 0.05$, t-test.
†Differs from healthy control value, $p < 0.0000001$, t-test.
Ham-D = Hamilton Depression Scale; MMSE = Mini-Mental State Examination; DRS = Dementia Rating Scale; ADAS-Cog = Alzheimer's Disease Assessment Scale-Cognitive subscale.

region of interest (ROI) analysis to compare cerebral SPECT images obtained with ^{99m}Tc-HMPAO and ^{99m}Tc-ECD in the same sample of AD patients and age-matched healthy control subjects. In the course of that analysis, we used receiver operating characteristic (ROC) analysis to examine the ability of the two tracers to correctly classify AD patients and control subjects.

MATERIALS AND METHODS

Subjects

The study population consisted of 24 patients with probable AD and 13 healthy control subjects whose characteristics are displayed in Table 1. Patients were recruited from among those participating in a trial of an investigational cognitive enhancing drug (and underwent SPECT imaging before starting active medication); control subjects were all spouses of participating AD patients. The patients were diagnosed as having probable AD according to standard criteria (*24*). Other causes of dementia were excluded through a comprehensive evaluation, including medical history, physical and neurological examinations, serum chemistries, thyroid function studies, complete blood count, B12, folate, VDRL, urinalysis, electrocardiogram, chest radiograph, and electroencephalogram. In addition, brain MRI was performed in all patients with a 1.5-tesla General Electric Signa scanner (Milwaukee, WI). Generalized atrophy was observed in 20/24 patients (mild-to-severe) and 5/13 control subjects (mild-to-moderate). Periventricular white matter lesions were observed in 17/24 patients (mild-to-moderate) and 9/13 control subjects (mild-to-moderate). At the time of SPECT scanning, no patients or control subjects were taking medications known to alter cerebral blood flow.

Subjects were excluded if they scored > 14 on the Hamilton Depression Scale (*25*). AD patients were excluded if the had a Hachinski ischemia score (*26*) > 4. AD subjects were required to score ≤ 24 and ≥ 14 (mild-to-moderate severity range) and healthy subjects ≥ 27 on the Mini Mental State Examination (*27*).

Other neuropsychological testing administered for subject characterization (Table 1) included the Dementia Rating Scale (DRS) (*28*), the cognitive subscale of the Alzheimer's Disease Assessment Scale (ADAS-Cog) (*29*), and the Wechsler Adult Intelligence Scale-Revised (WAIS-R) (*30*). Patients and healthy control subjects differed significantly in all cognitive neuropsychological measures ($p \ll 0.0001$, t-test; Table 1). All patients and control subjects had at least 8 yr of education.

Two AD patients and one healthy control have died and received brain autopsies since study participation. Histopathology confirmed clinical diagnosis in all three cases.

Data Acquisition

The ^{99m}Tc-HMPAO scan always preceded the ^{99m}Tc-ECD scan because the latter scan was performed as part of a corporate-sponsored IND protocol that precluded concurrent studies. The average time between ^{99m}Tc-HMPAO and ^{99m}Tc-ECD scans was 13.6 ± 6.5 days (range 7–33 days) for the patients and 12.5 ± 6.4 days (range 2–27 d) for the control subjects. The radiochemical purity of each tracer was determined according to the methods outlined in the package inserts. The radiochemical purity of ^{99m}Tc-HMPAO was 92.1% ± 3.9% and of ^{99m}Tc-ECD was 97.9% ± 1.5%. The ^{99m}Tc-HMPAO used was the original nonstabilized preparation.

Technetium-99m-HMPAO (20.1 ± 0.8 mCi) or ^{99m}Tc-ECD (20.4 ± 0.9 mCi) was injected intravenously in the nuclear medicine suite at Yale New Haven Hospital. At the time of injection, subjects were supine with eyes and ears uncovered in a dimly lit room. Quiet was maintained for 5 min postinjection.

The postinjection interval (PII) for each tracer was chosen according to clinical practice standards. PII has typically been at least 30 min for ^{99m}Tc-ECD (*31–33*) compared to only 10 to 20 min for ^{99m}Tc-HMPAO (*3,4*), based on evidence that ^{99m}Tc-ECD, but not ^{99m}Tc-HMPAO, undergoes washout of blood and facial activity at longer PIIs (*17,22*). Accordingly, scanning began on average 11.5 ± 2.8 min (range 10 to 25 min) after injection for ^{99m}Tc-HMPAO and 41.8 ± 10.1 min (range 25 to 67 min) for ^{99m}Tc-ECD. Acquisition time was 30 min for each tracer.

SPECT data were acquired with the multislice brain dedicated CERASPECT camera (Digital Scintigraphics, Waltham, MA) (*34,35*) with a resolution of 7–8 mm FWHM in all three axes. Data were acquired in 120 projections with a 360-degree rotation of the collimators. Two pulse-height analyzer windows were used, one set at the photopeak (140 ± 14 keV) and the other set to acquire scatter information (112–126 keV). After data acquisition, collimator and crystal corrections were performed on each dataset. A combined set of projections was then calculated by subtracting 70% of the scatter projections, filtered to remove the forward scatter component, from the photopeak projections. The projections were prefiltered using a Butterworth filter (cutoff = 0.10 cycles/cm; power factor = 10).

Image Analysis

SPECT images were analyzed by two investigators (HL and RR) blinded to subject identity and radiopharmaceutical. Analysis of each subject's two scans was performed simultaneously to optimize anatomic co-localization between the two scan conditions. Reconstructed slices were displayed on a 128 × 128 matrix (1.67 x 1.67 mm pixel size) as a set of 64 transaxial slices (1.67 mm slice thickness). SPECT data were rotated and resliced to correct for deviations from the canthomeatal plane. Five standard transaxial slices 6.67-mm thick were then created by digitally summing groups of 4 of the 1.67-mm slices at defined anatomical levels (Fig. 1): (a) maximal cerebellar activity; (b) maximal thalamic activity; (c) lowest central activity (superior to thalamus and basal ganglia and inferior to midline gray matter); two additional high cortical slices (d) and (e) were chosen approximately 10 and 20 mm above the (c) slice. The five standard slices were thus situated

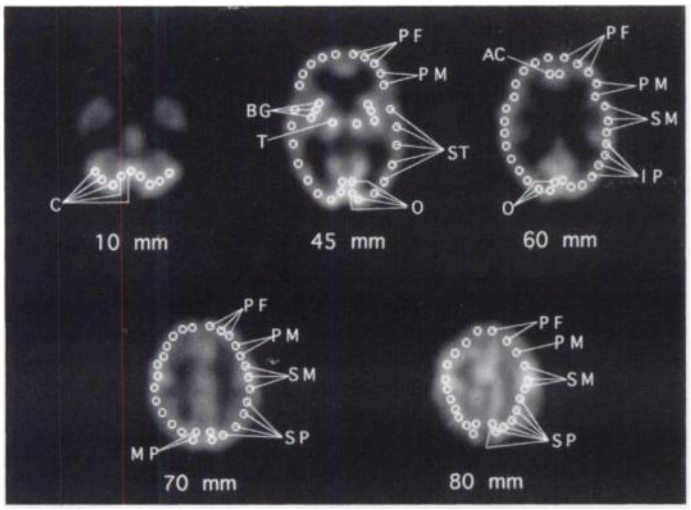

FIGURE 1. Region of interest (ROI) template used in the SPECT analysis. The millimeter specification below each slice is the distance above the canthomeatal plane. C = cerebellum; BG = basal ganglia; T = thalamus; PF = prefrontal cortex; PM = premotor cortex; ST = superior temporal cortex; O = occipital cortex; AC = anterior cingulate cortex; SM = sensorimotor cortex; IP = inferior parietal cortex; MP = medial parietal cortex; SP = superior parietal cortex.

approximately 10, 45, 60, 70 and 80 mm above the canthomeatal plane. Attenuation correction was performed using a Chang zero-order method (attenuation coefficient $\mu = 0.15$ cm^{-1}) within an ellipse drawn around the skull. The same attenuation ellipses were used within subjects for ^{99m}Tc-HMPAO and ^{99m}Tc-ECD scans at each anatomic level.

A ROI template (Fig. 1) was constructed based loosely on that of Kumar et al. (*36*) for studies of AD using ^{18}F-2-fluoro-2-deoxy-D-glucose (FDG) in AD. This template comprised 135 circular ROIs of preset area (21 pixels or 58.33 mm^2), representing 12 anatomic structures, and distributed evenly throughout each region and centrally in subcortical regions. The ROIs in the template were visually adjusted using a standard brain atlas (*37*) to best fit individual anatomy based on landmarks in the SPECT image.

Statistical Analysis

Count densities for anatomic structures were obtained by averaging the values in circular ROIs across all slices in which the structures appeared. For example, the count density for the prefrontal cortex was obtained by averaging the count densities in prefrontal ROIs across the 45-, 60-, 70- and 80-mm levels above the canthomeatal plane (Fig. 1). For each radiopharmaceutical, a final count density was determined for the 12 structures (listed in Table 2) for each subject by averaging the values obtained by the two image analysts.

The principal outcome measure for the present study was the ratio of count densities in structures "typically affected" by AD (parietal and temporal association cortices) to those in relatively "unaffected" structures (defined as cerebellum, basal ganglia, thalamus, occipital cortex, and sensorimotor cortex). The selection of structures as "typically affected" or "unaffected" is based on evidence from both neuropathological studies (*38–40*) as well as PET studies of cerebral blood flow (*41*) and glucose metabolism (*36,41–44*). This composite ratio is similar to that used by Herholz et al. (*43,44*) in FDG studies of AD but differs by excluding frontal association cortex from the "typically affected" structures and including thalamus in the "unaffected" structures. This ratio is hereafter referred to as *R*.

Although "typically affected" and relatively "unaffected" structures in *R* were selected a priori, an analysis was undertaken a posteriori to determine the appropriateness of this selection for each tracer. The ^{99m}Tc-HMPAO and ^{99m}Tc-ECD SPECT methods used (in the absence of measurement of the arterial input function) do not permit absolute quantitation of CBF. However, by assuming that the arterial input function and the clearance for each tracer is constant within subjects across brain regions, then count density data can be used to compare different brain regions within a given subject sample. For this analysis, the mean cpm_{AD} (expressed as a percentage of mean $cpm_{Control}$) was used to identify regions with relatively normal and abnormal tracer uptake in the AD patients. The results of this analysis are displayed in Table 2 and validate the choice of "unaffected" structures.

Inter-rater reliability was measured for *R* for the two image analysts using Pearson's product moment correlation coefficient (Pearson's *r*). For each subject, a final value of *R* was computed for each radiopharmaceutical by averaging the *R* values of the two image analysts. The relationship between *R* values for ^{99m}Tc-HMPAO and ^{99m}Tc-ECD was also compared using Pearson's *r*.

The effect of radiopharmaceutical and diagnostic group on *R* was determined by two-way analysis of variance (ANOVA) with repeated measures on radiopharmaceutical. Receiver operating characteristic (ROC) curves were calculated by varying the threshold of *R* to compare the diagnostic accuracy of ^{99m}Tc-HMPAO and

TABLE 2
Count Density Data Showing Rank Order of Preserved Tracer Uptake for 12 Brain Structures in Alzheimer's Disease

	^{99m}Tc-ECD					^{99m}Tc-HMPAO				
	Control		Alzheimer's			Control		Alzheimer's		
Brain structure	Mean	s.d.	Mean	s.d.	% Control	Rank	Mean	s.d.	Mean	s.d.	% Control	Rank
Cerebellum	168.77	± 50.45	179.18	± 74.24	106.2%	1	180.88	± 36.96	194.07	± 55.30	107.3%	1
Basal ganglia	158.11	± 44.10	161.78	± 63.24	102.3%	2	176.61	± 36.77	184.06	± 54.83	104.2%	3
Thalamus	194.39	± 51.25	193.34	± 72.55	99.5%	3	211.66	± 38.60	222.00	± 62.70	104.9%	2
Sensorimotor	140.93	± 39.55	137.73	± 62.06	97.7%	4	144.39	± 31.87	146.27	± 46.98	101.3%	5
Occipital	172.31	± 49.57	165.03	± 75.50	95.8%	5	162.57	± 36.26	165.80	± 56.04	102.0%	4
Prefrontal	140.02	± 35.15	133.14	± 49.95	95.1%	6	152.02	± 27.73	148.81	± 40.21	97.9%	6
Anterior cingulate	150.48	± 40.86	140.74	± 56.86	93.5%	7	166.07	± 36.00	155.80	± 44.35	93.8%	9
Premotor	145.99	± 38.77	135.70	± 53.98	92.9%	8	154.88	± 29.95	150.30	± 42.83	97.0%	7
Superior temporal	147.34	± 42.48	132.84	± 60.35	90.2%	9	152.71	± 33.90	145.01	± 48.03	95.0%	8
Medial parietal	166.57	± 48.22	148.25	± 66.75	89.0%	10	168.15	± 40.35	155.53	± 54.60	92.5%	10
Inferior parietal	145.47	± 42.52	123.81	± 59.10	85.1%	11	150.73	± 36.86	137.99	± 47.42	91.5%	11
Superior parietal	146.13	± 41.43	123.87	± 56.14	84.8%	12	149.84	± 32.71	136.50	± 46.09	91.1%	12

$\%Control = (Mean_{Alzheimer's}/Mean_{Control}) * 100\%$.

TABLE 3
rCBF Ratios in Association Cortices for Patients and Controls Using Both Tracers

	^{99m}Tc-HMPAO			^{99m}Tc-ECD		
	Control	Alzheimer's		Control	Alzheimer's	
	Mean s.d.	Mean s.d.	% Control	Mean s.d.	Mean s.d.	% Control
Anterior cingulate						
Left	1.03 ± 0.08	0.92 ± 0.12	90.0%	0.96 ± 0.09	0.89 ± 0.13	92.5%
Right	1.01 ± 0.08	0.94 ± 0.12	92.9%	0.94 ± 0.10	0.89 ± 0.12	94.9%
Prefrontal						
Left	0.94 ± 0.04	0.90 ± 0.07	95.5%	0.89 ± 0.05	0.86 ± 0.08	96.6%
Right	0.93 ± 0.04	0.89 ± 0.07	95.1%	0.89 ± 0.05	0.85 ± 0.07	95.5%
Premotor						
Left	0.96 ± 0.04	0.90 ± 0.07	93.2%	0.92 ± 0.03	0.86 ± 0.08	93.9%
Right	0.94 ± 0.04	0.90 ± 0.07	95.4%	0.92 ± 0.04	0.86 ± 0.07	93.6%
Superior temporal						
Left	0.93 ± 0.05	0.86 ± 0.05	92.5%	0.91 ± 0.05	0.83 ± 0.06	91.1%
Right	0.94 ± 0.03	0.85 ± 0.07	90.9%	0.93 ± 0.04	0.84 ± 0.08	89.8%
Inferior parietal						
Left	0.92 ± 0.05	0.81 ± 0.07	88.6%	0.90 ± 0.05	0.78 ± 0.07	86.5%
Right	0.92 ± 0.04	0.81 ± 0.09	88.2%	0.92 ± 0.04	0.77 ± 0.10	83.9%
Medial parietal						
Left	1.04 ± 0.06	0.93 ± 0.08	89.4%	1.05 ± 0.07	0.94 ± 0.09	90.0%
Right	1.01 ± 0.08	0.90 ± 0.09	88.9%	1.04 ± 0.08	0.92 ± 0.10	89.1%
Superior parietal						
Left	0.91 ± 0.04	0.81 ± 0.07	89.4%	0.91 ± 0.04	0.78 ± 0.07	86.4%
Right	0.93 ± 0.04	0.80 ± 0.08	86.0%	0.92 ± 0.04	0.77 ± 0.09	83.8%
Parietotemporal (R)	0.93 ± 0.03	0.83 ± 0.06	88.8%	0.93 ± 0.02	0.81 ± 0.06	86.7%

Values normalized to relatively "unaffected" regions (cerebellum, basal ganglia, thalamus, sensorimotor cortex, occipital cortex). %Control = $(\text{Mean}_{\text{Alzheimer's}}/\text{Mean}_{\text{Control}}) * 100\%$.

^{99m}Tc-ECD. Wilcoxon statistics were used to assess significance (*45*). All statistical analyses were performed using the SYSTAT software package (SYSTAT, Inc., Evanston, IL).

RESULTS

Technetium-99m-HMPAO and ^{99m}Tc-ECD demonstrated a similar regional pattern of tracer uptake in the AD patients (Table 2). The largest decreases in activity in AD (in terms of percentage of control values) were found in the superior, inferior, and medial parietal cortices followed by the superior temporal cortex for ^{99m}Tc-ECD and the anterior cingulate followed by the superior temporal cortex for ^{99m}Tc-HMPAO. The least abnormal structures for both tracers were the cerebellum, thalamus, basal ganglia, occipital cortex, and sensorimotor cortex; although the relative order of these structures differed slightly for the two tracers. This a posteriori analysis thus provides further support for the regions chosen as "typically affected" and relatively "unaffected" for derivation of *R*. The large variability in these data is consistent with the fact that these are un-normalized count density data. Table 3 presents rCBF ratio data normalized to the five "unaffected" structures for the remaining seven association cortices.

The two image analysts showed very high inter-rater reliability for the *R* value ($r = 0.98$, $n = 37$, $p \ll 0.0001$). Their *R* values were then averaged for subsequent analyses. *R* values for the two radiopharmaceuticals were highly correlated ($r = 0.95$, $n = 37$, $p \ll 0.0001$) as displayed in Figure 2.

The scatter data for *R* are displayed in Figure 3. They reveal significant differences between diagnostic groups ($F = 43.77$; $df = 1,35$; $p \ll 0.0001$) and radiopharmaceuticals ($F = 10.03$; $df = 1,35$; $p = 0.003$). There was also a significant interaction between diagnostic group and tracer ($F = 4.71$; $df = 1,35$; $p = 0.04$), with ^{99m}Tc-ECD demonstrating better separation of *R* values between AD patients and control subjects than ^{99m}Tc-HMPAO. Figure 4 displays a representative comparison of ^{99m}Tc-HMPAO and ^{99m}Tc-ECD images from an individual AD patient.

ROC curves for ^{99m}Tc-HMPAO in comparison to ^{99m}Tc-ECD are displayed in Figure 5. Thirty-six of the 37 subjects

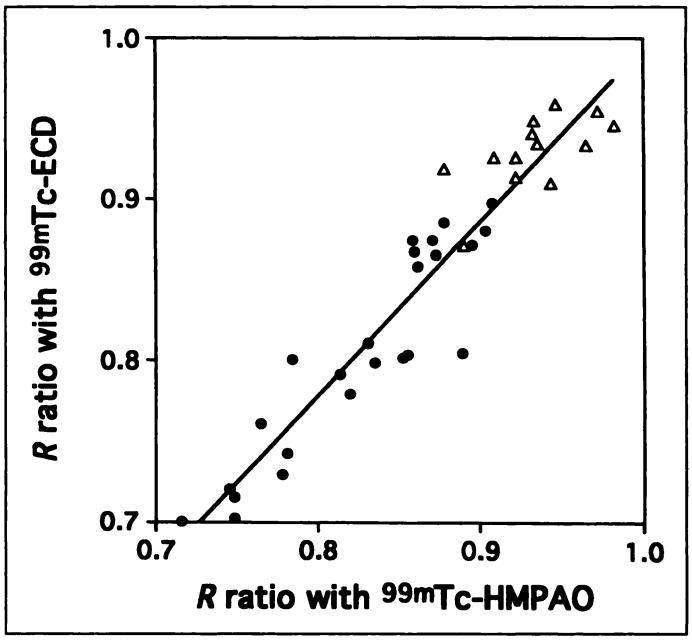

FIGURE 2. Relationship between rCBF ratios (*R*) in parietotemporal region for individual AD patients (n = 24) and control subjects (n = 13) for ^{99m}Tc-HMPAO and ^{99m}Tc-ECD. Values represent count densities normalized to regions relatively "unaffected" in AD (cerebellum, basal ganglia, thalamus, occipital cortex, and sensorimotor cortex). Closed circles denote AD patients and open triangles control subjects. *R* values for ^{99m}Tc-HMPAO and ^{99m}Tc-ECD) were highly correlated ($r = 0.95$, $n = 37$, $p \ll 0.0001$).

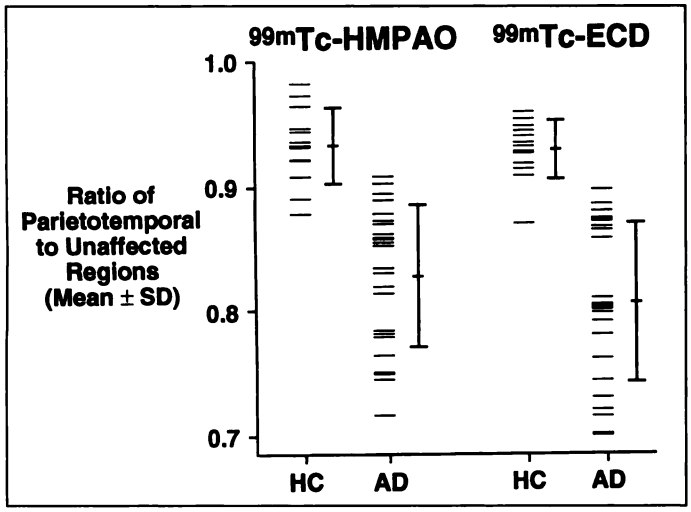

FIGURE 3. Scatterplot of rCBF ratios (*R*) in parietotemporal region for individual AD patients (n = 24) and control subjects (n = 13) for ^{99m}Tc-HMPAO and ^{99m}Tc-ECD. Values represent count densities normalized to regions relatively "unaffected" in AD (cerebellum, basal ganglia, thalamus, occipital cortex, and sensorimotor cortex). Each dash denotes an individual subject. Analysis of variance revealed a significant interaction between diagnostic group and radiopharmaceutical (F = 4.71; df = 1,35; p = 0.04), with ^{99m}Tc-ECD demonstrating better separation of *R* values between AD patients and control subjects than ^{99m}Tc-HMPAO.

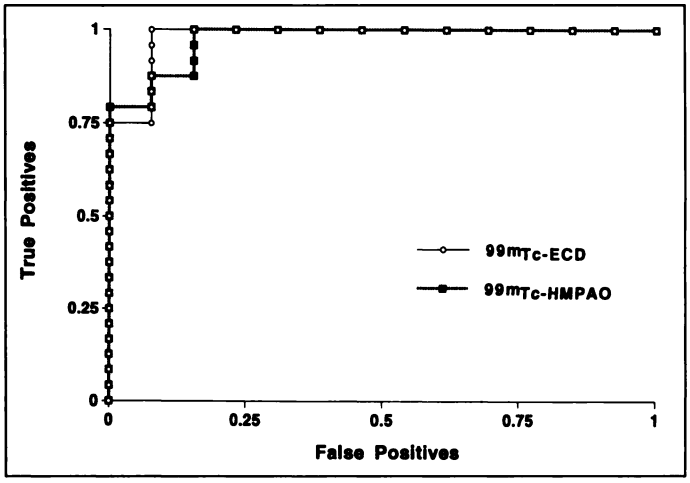

FIGURE 5. Receiver operating characteristic (ROC) curves of the diagnostic accuracy of the composite ratio *R* ("typically affected" to relatively "unaffected" regions) for ^{99m}Tc-HMPAO and ^{99m}Tc-ECD. There was no significant difference in the ability of the two tracers to correctly classify AD patients and control subjects. The area under the ROC curve covered 98.1% (s.e. 2.1%) for ^{99m}Tc-ECD and 97.4% (s.e. 2.2%) for ^{99m}Tc-HMPAO.

(97.3%) were classified correctly at a threshold of 0.903 for the composite ratio *R* for ^{99m}Tc-ECD; whereas 35 of the 37 subjects (94.6%) were classified correctly at a threshold of 0.909 for *R* for ^{99m}Tc-HMPAO. Corresponding sensitivity (% true-positives) was 100% and specificity (% true-negatives) was 92.3% for ^{99m}Tc-ECD. Sensitivity was 100% and specificity 84.6% for ^{99m}Tc-HMPAO. The area under the ROC curve covered 98.1% (s.e. 2.1%) for ^{99m}Tc-ECD and 97.4% (s.e. 2.2%) for ^{99m}Tc-HMPAO. This small difference was not statistically significant (Z = 0.46, p = 0.65) (*45*).

DISCUSSION

This study compared cerebral SPECT images obtained with ^{99m}Tc-HMPAO and ^{99m}Tc-ECD in the same sample of AD patients and age-matched control subjects. The results of this study suggest significantly greater contrast between "typically affected" and relatively "unaffected" brain structures in AD for ^{99m}Tc-ECD than for ^{99m}Tc-HMPAO. ^{99m}Tc-ECD (PII = 41.8 ± 10.1 min) demonstrated better separation of *R* values between AD patients and control subjects than ^{99m}Tc-HMPAO (PII = 11.5 ± 2.8 min). Whether the magnitude of this difference is clinically meaningful remains uncertain. The lack of a significant difference by ROC analysis in the ability of the two tracers to correctly classify patients and control subjects may reflect the limited statistical power of the present study to detect diagnostic differences.

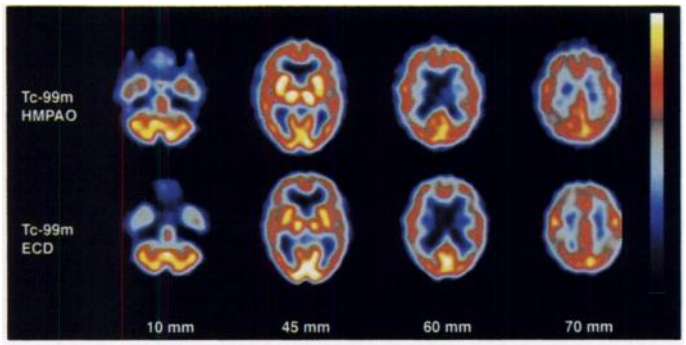

FIGURE 4. Cerebral SPECT images for a 67-yr-old woman with probable AD using ^{99m}Tc-HMPAO and ^{99m}Tc-ECD. The ^{99m}Tc-ECD images demonstrate greater contrast than ^{99m}Tc-HMPAO between "typically affected" and relatively "unaffected" brain regions. This difference is most evident in the 70-mm slice in the comparison between superior parietal association cortex (affected) and sensorimotor cortex (relatively unaffected). The slice 80 mm above the canthomeatal plane is not shown.

Most striking was the high diagnostic accuracy demonstrated by both tracers (^{99m}Tc-ECD: 97.3%; ^{99m}Tc-HMPAO: 94.6%). These values are comparable to those reported by Herholz et al. (*43*) using a similar composite ratio comparing AD patients and healthy control subjects with PET and FDG (diagnostic accuracy = 95.8%). As in that report, we did not confirm diagnosis by autopsy in the present study. However, we performed extensive clinical evaluation to implement standard diagnostic criteria (*24*) and to exclude other etiologies of dementia. Such methods have been reported do achieve a diagnostic accuracy approaching 100% (*46*).

Interpretation of Image Differences

These results are consonant with previous comparative studies of the two agents in chronic stroke (*18–20*) and mixed neurological samples (*21*) in which ^{99m}Tc-ECD showed higher lesion-to-normal tissue contrast than ^{99m}Tc-HMPAO. The greater affected-to-unaffected tissue contrast for ^{99m}Tc-ECD in AD likely accrues from the same pharmacokinetic factors that have been noted in other healthy and neurological samples. Technetium-99m-ECD is cleared from the blood more rapidly than ^{99m}Tc-HMPAO and demonstrates less background facial uptake (*17,22*). Such differences would be expected to favor the functioning of the reconstruction algorithm for ^{99m}Tc-ECD (*22,47*).

The superior image quality of ^{99m}Tc-ECD appears to be less a function of brain kinetics since, as reported by Pupi et al. (*22*), the values of K_i for the two tracers are comparable throughout a clinical perfusion range. The greater cerebral extraction (E) for ^{99m}Tc-HMPAO (*48*) is probably compensated by a greater retention fraction (R) $[k_3/(k_2+k_3)]$ for ^{99m}Tc-ECD which derives from a smaller rate of backdiffusion (k_2) (*49*). Both tracers are known to underestimate cerebral blood flow in the high flow range (*13,15,19,48,50*). Greater understanding of these issues is needed before conclusions are drawn about their significance in intrasubject differences in SPECT image quality.

Limitations of Present Study

The present study has certain limitations in its design and the interpretation of its results. These include: (a) the small sample size (for ROC analysis), (b) the absence of autopsy confirmation of clinical diagnosis in most cases and (c) the absence of a counterbalanced sequence: the ^{99m}Tc-HMPAO scan always preceded ^{99m}Tc-ECD scan. We cannot exclude confounding order effects, although we consider these unlikely.

A more important limitation is the significantly longer PII for ^{99m}Tc-ECD (41.8 ± 10.1 min) than for ^{99m}Tc-HMPAO (11.5 ± 2.8 min). We attempted to optimize scanning conditions by following clinical practice standards for PII for each tracer. For ^{99m}Tc-HMPAO, PII in clinical practice has typically ranged from about 10 min (*3*) to 20 min (*4*). For ^{99m}Tc-ECD, PII in clinical practice has usually been at least 30 min (*31–33*) and sometimes as long as 120 min (*51*). Devous et al. (*15*) have advocated a PII of at least 45 min for ^{99m}Tc-ECD to avoid the early phase of rapid clearance and to await the prolonged stable period of slow clearance. Accordingly, some previous comparative studies of the two tracers have used a longer PII for ^{99m}Tc-ECD (e.g., 10 min for ^{99m}Tc-HMPAO and 30 min for ^{99m}Tc-ECD) (*19*).

We cannot exclude the possibility that the greater affected-to-unaffected tissue contrast found in the present study for ^{99m}Tc-ECD derived in part from the longer PII used. However, previous evidence suggests that ^{99m}Tc-ECD, but not ^{99m}Tc-HMPAO, can profit from the washout of blood and facial activity at the longer PII. Pupi et al. (*22*) reported that in serial SPECT acquisitions started 35 and 60 min postinjection, ^{99m}Tc-ECD but not ^{99m}Tc-HMPAO demonstrated continued washout of background activity, while both tracers showed stable brain activity. Similarly, Léveillé et al. (*17*) found that brain-to-soft-tissue activity ratios continued to increase with time for ^{99m}Tc-ECD, but not ^{99m}Tc-HMPAO. Moreover, Anderson et al. (*13*) demonstrated that image contrast with ^{99m}Tc-HMPAO in neurological patients did not increase significantly from 10 min to 5 hr postinjection. It seems unlikely, therefore, that a longer PII would benefit ^{99m}Tc-HMPAO, given that total brain counts would be sacrificed. Previous comparative studies that have used comparable PIIs for the two tracers have still found greater lesion-to-normal tissue contrast for ^{99m}Tc-ECD than ^{99m}Tc-HMPAO (*18,21*). Nonetheless, future comparative studies should examine the effect of PII on image quality in AD.

The ^{99m}Tc-HMPAO used in the present study was the original nonstabilized formulation. In the newer preparation, methylene blue is reported to enhance the in vitro stability of ^{99m}Tc-HMPAO without producing new chemical entities or altering in vivo imaging characteristics (Amersham, Ltd., *personal communication*). Therefore, our results will likely apply to the newer stabilized product as well. However, careful comparative studies may be necessary to verify the diagnostic comparability of the two preparations.

CONCLUSION

The two ^{99m}Tc-based SPECT brain perfusion agents, ^{99m}Tc-HMPAO and ^{99m}Tc-ECD, demonstrate a similar regional pattern of tracer uptake in AD. However, ^{99m}Tc-ECD shows greater contrast than ^{99m}Tc-HMPAO between affected and unaffected brain structures in AD when patients are compared to age-matched control subjects. In the present sample, this difference did not yield a significant advantage for ^{99m}Tc-ECD in classifying patients and control subjects. The high diagnostic accuracy exhibited by both tracers supports the continued investigation of SPECT as a diagnostic tool in AD.

ACKNOWLEDGMENTS

We thank George Zubal, PhD for consultation on SPECT instrumentation; Sami Zoghbi, PhD for consultation on radiochemistry; and Susan Broshjeit for technical assistance. This research was supported by United States Public Health Service grant R03-MH47459. The radiopharmaceuticals, Ceretec and Neurolite, were supplied by Amersham, Ltd., Amersham, England, and DuPont-Merck Pharmaceuticals, Inc., Billerica, MA, respectively.

REFERENCES

1. Johnson KA, Mueller ST, Walshe TM, English RJ, Holman BL. Cerebral perfusion imaging in Alzheimer's disease. *Arch Neurol* 1987;44:165–168.
2. Jagust WJ, Budinger TF, Reed BR. The diagnosis of dementia with single-photon emission computed tomography. *Arch Neurol* 1987;44:258–262.
3. Holman BL, Johnson KA, Gerada B, Carvalho PA, Satlin A. The scintigraphic appearance of Alzheimer's disease: a prospective study using technetium-99m-HMPAO SPECT. *J Nucl Med* 1992;33:181–185.
4. Johnson KA, Kijewski MF, Becker JA, Garada B, Satlin A, Holman BL. Quantitative brain SPECT in Alzheimer's disease and normal aging. *J Nucl Med* 1993;34:2044–2048.
5. Bonte FJ, Tintner R, Weiner MF, Bigio EH, White III CL. Brain blood flow in the dementias: SPECT with histopathologic correlation. *Radiology* 1993;186:361–365.
6. Jobst KA. Alzheimer's disease is accurately diagnosed by combining ^{99m}Tc-HMPAO SPECT and temporal lobe oriented x-ray CT scans [Abstract]. *J Nucl Med* 1994; 35(suppl):20P.
7. Jobst KA, Hindley NJ, King E, Smith AD. The diagnosis of Alzheimer's disease: a question of image? *J Clin Psychiatry* 1994;55:22–31.
8. Neirinckx RD, Canning LR, Piper IM, et al. Technetium-99md,l-HM-PAO: A new radiopharmaceutical for SPECT imaging of regional cerebral blood perfusion. *J Nucl Med* 1987;28:191–202.
9. Sharp PF, Smith FW, Gemmell HG, et al. Technetium-99m-HMPAO stereoisomers as potential agents for imaging regional cerebral blood flow: human volunteer studies. *J Nucl Med* 1986;27:171–177.
10. Walovitch RC, Hill TC, Garrity ST, et al. Characterization of technetium-99m-L,L-ECD for brain perfusion imaging, part 1: pharmacology of technetium-99m-ECD in nonhuman primates. *J Nucl Med* 1989;30:1892–1901.
11. Léveillé J, Demonceau G, De Roo M, et al. Characterization of technetium-99m-L,L-ECD for brain perfusion imaging, part 2: biodistribution and brain imaging in humans. *J Nucl Med* 1989;30:1902–1910.
12. Vallabhajosula S, Zimmerman RE, Picard M, et al. Technetium-99m-ECD: a new brain imaging agent: in vivo kinetics and biodistribution studies in normal human subjects. *J Nucl Med* 1989;30:599–604.
13. Andersen AR, Friberg HH, Schmidt JF, Hasselbalch SG. Quantitative measurements of cerebral blood flow using SPECT and ^{99m}Tc-HMPAO compared to xenon-133. *J Cereb Blood Flow Metab* 1988;8:S69–S81.
14. Yonekura Y, Nishizawa S, Mukai T, et al. SPECT with [^{99m}Tc]-d,l-hexamethyl-propylene amine oxime (HMPAO) compared with regional cerevral blood flow measured by PET: effects of linearization. *J Cereb Blood Flow Metab* 1988;8:S82–S89.
15. Devous MDS, Payne JK, Lowe JK, Leroy RF. Comparison of technetium-99m-ECD to xenon-133 SPECT in normal controls and in patients with mild to moderate regional cerebral blood flow abnormalities. *J Nucl Med* 1993;34:754–761.
16. Orlandi C, Crane PD, Platts SH, Walovitch RC. Regional cerebral blood flow and distribution of [^{99m}Tc] ethyl cysteinate dimer in nonhuman primates. *Stroke* 1990;21: 1059–1063.
17. Léveillé J, Demonceau G, Walovitch RC. Intrasubject comparison between technetium-99m-ECD and technetium-99m-HMPAO in healthy human subjects. *J Nucl Med* 1992;33:480–484.
18. Matsuda H, Li YM, Higashi S, et al. Comparative SPECT study of stroke using ^{99m}Tc-ECD, ^{123}I-IMP,and ^{99m}Tc-HMPAO. *Clin Nucl Med* 1993;18:754–758.
19. Tsuchida T, Nishizawa S, Yonekura Y, et al. SPECT Images of technetium-99m-ethyl cysteinate dimer in cerebrovascular diseases: comparison with other cerebral perfusion tracers and PET. *J Nucl Med* 1994;35:27–31.
20. Moretti JL, Defer G, Cinotti L, Cesaro P, Vigneron N, Pethe C. Comparative tomoscintigraphic study of strokes using ^{99m}Tc-ECD, ^{99m}Tc-HMPAO and ^{123}I-IMP: preliminary results [Abstract]. *Eur J Nucl Med* 1988;14:311.
21. Castagnoli A, Borsato N, Bruno A, et al. SPECT brain imaging in chronic stroke and dementia: a comparison of ^{99m}Tc-ECD and ^{99m}Tc-HMPAO. In: Hartmann A, Hoyer S, Kuschinky W, eds. *Cerebral ischemia and dementia.* Stuttgart: Springer-Verlag; 1991:327–333.
22. Pupi A, Castagnoli A, De Cristofaro MR, Bacciottini L, Petti A. Quantitative comparison between ^{99m}Tc-HMPAO and ^{99m}Tc-ECD: measurement of arterial input and brain retention. *Eur J Nucl Med* 1994;21:124–130.
23. Tanada S, Murase K, Inoue T, et al. Comparison of kinetics in brain tumors between ^{99m}Tc-ECD and ^{99m}Tc-HMPAO with dynamic brain SPECT and compartment model [Abstract]. *J Nucl Med* 1992;33(suppl):969.
24. McKhann G, Drachman D, Folstein M, Katzman R, Price D, Stadlan EM. Clinical diagnosis of Alzheimer's disease: report of the NINCDS-ADRDA work group under the auspices of Department of Health and Human Services Task Force on Alzheimer's disease. *Neurology* 1984;34:939–944.
25. Hamilton M. A rating scale for depression. *J Neurol Neurosurg Psych* 1960;23:56–62.
26. Hachinski VC, Iliff LD, Zilhka E, et al. Cerebral blood flow in dementia. *Arch Neurol* 1975;32:632–637.
27. Folstein MF, Fostein SE, McHugh PR. "Mini-mental state": a practical method for

grading the cognitive state of patients for the clinician. *J Psychiatr Res* 1975;12:189–198.
28. Mattis S. Mental status examination for organic mental syndrome in the elderly patient. In: Bellack L, Karasu TB, eds. *Geriatric psychiatry.* New York: Grune & Stratton; 1976:77–121.
29. Rosen WG, Mohs RC, Davis KL. A new rating scale for Alzheimer's disease. *Am J Psychiatry* 1984;141:1356–1364.
30. Wechsler D. *Wechsler adult intelligence scale—revised.* New York: Psychological Corporation; 1981.
31. Lassen NA, Sperling B. Technetium-99m-bicisate reliably images CBF in chronic brain diseases but fails to show reflow hyperemia in subacute stroke: report of a multicenter trial of 105 cases comparing ^{133}Xe and ^{99m}Tc-biscisate (ECD, Neurolite) measured by SPECT on same day. *J Cereb Blood Flow Metab* 1994;14:S44–S48.
32. Yonekura Y, Tsuchida T, Sadato N, et al. Brain perfusion SPECT with ^{99m}Tc-biscisate: comparison with PET measurement and linearization based on permeablility-surface area product model. *J Cereb Blood Flow Metab* 1994;14:S58–S65.
33. Holm S, Madsen PL, Sperling B, Lassen NA. Use of ^{99m}Tc-bicisate in activation studies by split-dose technique. *J Cereb Blood Flow Metab* 1994;14:S115–S120.
34. Genna S, Smith AP. The development of ASPECT, an annular single crystal brain camera for high efficiency SPECT. *IEEE Trans Nucl Sci* 1988;NS-35:654–658.
35. Holman BL, Carvalho PA, Zimmerman RE, et al. Brain perfusion SPECT using an annular single crystal camera: initial clinical experience. *J Nucl Med* 1990;31:1456–1461.
36. Kumar A, Schapiro MB, Grady C, et al. High-resolution PET studies in Alzheimer's disease. *Neuropsychopharmacology* 1991;4:35–46.
37. Matsui T, Hirano A. *An atlas of the human brain for computerized tomography.* Tokyo: Igaku-Shoin, Ltd; 1978.
38. Brun A, Englund E. Regional pattern of degeneration in Alzheimer's disease: neuronal loss and histopathological grading. *Histopathology* 1981;5:549–564.
39. Pearson RCA, Esiri MM, Hiorns RW, Wilcock GK, Powell TPS. Anatomical correlated of the distribution of the pathological changes in the neocortex in Alzheimer disease. *Proc Natl Acad Sci* 1985;82:4531–4534.
40. Rogers J, Morrison JH. Quantitataive morphology and regional and laminar distributions of senile plaques in Alzheimer's disease. *J Neurosci* 1985;5:2801–2808.
41. Fukuyama H, Ogawa M, Yamauchi H, et al. Altered cerebral energy metabolism in Alzheimer's disease: a PET study. *J Nucl Med* 1994;35:1–6.
42. Kushner M, Tobin M, AlaviA, et al. Cerebellar glucose consumption in normal and pathologic states using fluorine-18-FDG and PET. *J Nucl Med* 1987;28:1667–1670.
43. Herholz K, Perani D, Salmon E, et al. Comparability of FDG-PET studies in probable Alzheimer's disease. *J Nucl Med* 1993;34:1460–1466.
44. Herholz K, Adams R, Szelies B, Grond M, Heiss W-D. Criteria for the diagnosis of Alzheimer's disease with positron emission tomography. *Dementia* 1990;1:156–164.
45. Hanley JA, McNeil BJ. A method of comparing the areas under receiver operating characteristic curves derived from the same cases. *Radiology* 1983;148:839–843.
46. Morris J, McKeel D, Fulling K, Torack R, Berg L. Validation of clinical diagnostic criteria for Alzheimer's disease. *Ann Neurol* 1988;24:17–22.
47. Budinger TF, Derenzo SE, Greenberg WL, Guilberg GT. Quantitative potentials of dynamic emission computed tomography. *J Nucl Med* 1978;19:309–315.
48. Di Rocco RJ, Silva DA, Kuczynski BL, et al. The single-pass cerebral extraction and capillary permeability-surface area product of several putative cerebral blood flow imaging agents. *J Nucl Med* 1993;34:641–648.
49. Murase K, Tanada S, Inoue T, et al. Kinetic behavior of ^{99m}Tc-ECD in the human brain using compartment analysis and dynamic SPECT: comparison with ^{99m}Tc-HMPAO [Abstract]. *J Nucl Med* 1992;33(suppl):909.
50. Murase K, Tanada S, Inoue T, et al. Measurement of the blood-brain permeability of ^{123}I-IMP, ^{99m}Tc-HMPAO and ^{99m}Tc-ECD in the human brain using compartment model analysis and dynamic SPECT [Abstract]. *J Nucl Med* 1991;32(suppl):911.
51. Moretti JL, Defer G, Tamgac F, Weinmann P, Belin C, Cesaro P. Comparison of brain SPECT using ^{99m}Tc-bicisate (L,L-ECD) and [^{123}I]IMP in cortical and subcortical strokes. *J Cereb Blood Flow Metab* 1994;14:S84–S90.

Brain SPECT Evaluation of Patients with Pure Photosensitive Epilepsy

L. Özlem Kapucu, Kivilcim Gücüyener, Gülin Vural, Gülsen Köse, Ayse Bora Tokçaer, Bülent Turgut and Mustafa Ünlü
Departments of Nuclear Medicine, Pediatric Neurology and Neurology, Gazi University; and Department of Pediatric Neurology, Social Security Hospital, Ankara, Turkey

This study was performed to determine the utility of ^{99m}Tc-HMPAO brain SPECT in evaluating patients with pure photosensitive epilepsy. **Methods:** Seven patients (2 boys, 5 girls), aged 8 to 15 yr (mean 11.1 ± 2.5 yr), were studied. All patients underwent a detailed neurologic examination, interictal and ictal EEGs, CT and/or MRI and SPECT imaging. The baseline SPECT study was performed during the interictal period and the activation study was performed while the patients were having seizures provoked by watching television. **Results:** The baseline SPECT study showed that six of seven patients had relatively hypoperfused regions in their frontal lobes that could involve the neighboring parietal and temporal regions. The activation study revealed that all seven patients had relative hyperperfusion in these brain regions that were relatively hypoperfused in the baseline study. The side-to-side asymmetry indexes for these visually-interpreted rCBF abnormalities ranged from 3% to 6%. **Conclusion:** The relatively consistent pattern of frontal rCBF alterations suggests that frontal lobe functions were implicated in the evolution of photosensitivity-related seizures in patients with pure photosensitive epilepsy.

Key Words: pure photosensitive epilepsy; technetium-99m-HMPAO; brain SPECT; photic activation

J Nucl Med 1996; 37:1755–1759

Photosensitivity is found in 5% of epileptic patients and is associated with idiopathic generalized epilepsy, in which the prevalance may be as high as 25% (*1*). Forty percent of patients with seizures and photosensitivity have pure photosensitive epilepsy, in that all their attacks are visually precipitated and spontaneous seizures apparently do not occur (*1*). Seizures are commonly tonic-clonic (84% of this group, absences occur in 6%, partial seizures in 2.5% and myoclonic seizures in 1.5%). Nearly half of patients have a normal basic EEG, with abnormal activity occurring only on intermittant photic stimulation (IPS) (*1*).

The most common precipitant of seizures is television viewing. A more recent stimulus is the computer screen, although seizures may be induced by other sources of flickering light.

SPECT and PET functional neuroimaging techniques are used increasingly to diagnose seizure disorders, offering an accuracy of focus localization of approximately 90% for ictal and postictal studies in adult patients with complex partial seizures of temporal lobe origin (*2,3*). It has been suggested that ^{99m}Tc-hexamethylpropylene amine oxime (HMPAO) SPECT scanning may be useful in early diagnosis of partial status epilepticus, especially in cases where the initial EEG and clinical symptoms are difficult to interpret (*4*). However, little is known about abnormalities in cerebral perfusion or metabolism in generalized seizures and photosensitivity-induced seizure disorders have not been studied with functional neuroimaging. The aim of this study was to determine the utility of ^{99m}Tc-HMPAO brain SPECT in evaluating patients with pure photosensitive epilepsy.

Received Feb. 26, 1996; revision accepted March 6, 1996.
For correspondence or reprints contact: L. Özlem Kapucu, Department of Nuclear Medicine, Gazi University, Hoşdere Caddesi 3/17, Yukar[undot]i Ayranc[undot]i, 06540, Ankara, Turkey.